Tumor Biol. (2013) 34:695–704
DOI 10.1007/s13277-012-0597-7

RESEARCH ARTICLE

Oxidized alpha-1 antitrypsin as a predictive risk marker of opisthorchiasis-associated cholangiocarcinoma

Wassana Jamnongkan · Anchalee Techasen · Raynoo Thanan · Kunyarat Duenngai · Paiboon Sithithaworn · Eimorn Mairiang · Watcharin Loilome · Nisana Namwat · Chawalit Pairojkul · Puangrat Yongvanit

Received: 21 September 2012 / Accepted: 13 November 2012 / Published online: 28 November 2012
© International Society of Oncology and BioMarkers (ISOBM) 2012

Abstract The oxidized alpha-1 antitrypsin (ox-A1AT) is one modified form of A1AT, generated via oxidation at its active site by free radicals released from inflammatory cells which subsequently are unable to inhibit protease enzymes. The presence of ox-A1AT in human serum has been used as oxidative stress indicator in many diseases. As oxidative/nitrative damage is one major contributor in opisthorchiasis-driven cholangiocarcinogenesis, we determined A1AT and ox-A1AT expression in human cholangiocarcinoma (CCA) tissue using immunohistochemical staining and measured serum ox-A1AT levels by ELISA. A1AT and ox-A1AT were found to be expressed in the tumor of CCA patients. The group with high expression has a significant poor prognosis. Serum levels of ox-A1AT were also significantly higher in groups of patients with heavy *Opisthorchis viverrini* infection, advanced periductal fibrosis (APF) and CCA when compared with healthy controls ($P<0.001$). Odds ratio (OR) analysis implicated high ox-A1AT levels as a risk predictor for APF and CCA ($P<0.001$; OR=140.5 and 22.0, respectively). In conclusion, as APF may lead to hepatobiliary diseases and an increased risk of CCA development, our results identified ox-A1AT as a potential risk indicator for opisthorchiasis-associated CCA. This marker could now be explored for screening of subjects living in endemic areas where the prevalence of opisthorchiasis still remains high.

Keywords *Opisthorchis viverrini* · Oxidized alpha-1 antitrypsin · Risk marker · Cholangiocarcinoma · Periductal fibrosis

W. Jamnongkan · A. Techasen · R. Thanan · W. Loilome · N. Namwat · P. Yongvanit (✉)
Department of Biochemistry, Faculty of Medicine, Khon Kaen University, Khon Kaen 40002, Thailand
e-mail: puangrat@kku.ac.th

W. Jamnongkan · A. Techasen · R. Thanan · K. Duenngai · P. Sithithaworn · W. Loilome · N. Namwat · C. Pairojkul · P. Yongvanit
Liver Fluke and Cholangiocarcinoma Research Center, Khon Kaen University, Khon Kaen 40002, Thailand

K. Duenngai
Department of Biomedical Science Program, Graduate School, Khon Kaen University, Khon Kaen 40002, Thailand

P. Sithithaworn
Department of Parasitology, Faculty of Medicine, Khon Kaen University, Khon Kaen 40002, Thailand

E. Mairiang
Department of Radiology, Faculty of Medicine, Khon Kaen University, Khon Kaen 40002, Thailand

C. Pairojkul
Department of Pathology, Faculty of Medicine, Khon Kaen University, Khon Kaen 40002, Thailand

Introduction

Chronic inflammation induced by liver fluke (*Opisthorchis viverrini*) infection is the major risk factor for cholangiocarcinoma (CCA) in Northeastern Thailand. Although over time the prevalence of opisthorchiasis in the Northeast has gradually decreased due to mass treatment programs by the anti-trematode drug praziquantel, the incidence rate of CCA appears to remain unchanged in the endemic region [1–3]. Cholangiocarcinogenesis is a slow-progress tumor — which normally it takes at least 20–40 years for a patient to develop signs and symptoms, making CCA a highly mortal tumor,

because they are clinically silent in the majority of cases and are not detected early in most patients. Thus, the identification and validation of biomarkers that could be used in screening of subjects at high risk for *O. viverrini*-induced hepatobiliary disease and CCA are urgently needed.

The mechanism that governs the pathogenic effects of inflammation and immunity in liver fluke-associated cholangiocarcinogenesis has been recently reviewed [4]. Cellular damage caused by oxidative and nitrative stress during chronic infection appears to be a key event in *O. viverrini*-induced carcinogenesis which is further enhanced by an imbalanced oxidant/anti-oxidant system during re-infections [5]. We have demonstrated that infiltration of inflammatory cells triggered by repeated *O. viverrini* infection occurred earlier and more pronounced than after a single infection, resulting in altered liver enzyme activities [6, 7]. Hamsters which received repeated *O. viverrini* infections coupled with repeated praziquantel treatment showed an increased expression of apoptosis-related genes, which was associated with an increase in inflammatory cells surrounding the bile ducts [8, 9]. After *O. viverrini* infection, there was also a time-dependent increase in periductal fibrosis. The expression of matrix metalloproteinases (MMPs) is associated with an early phase inflammatory reaction while at the late phase tissue inhibitors of MMPs (TIMPs) expression may contribute to peribiliary fibrosis and liver injury [10]. Re-infection of subjects in endemic areas occurs more likely after praziquantel treatment and frequently leads to periductal fibrosis, hepatobiliary disease and subsequent CCA development [11, 12].

Several cellular proteins in human CCA tissue were found to be carbonylated that are generated *via* oxidative damage. Among those is alpha-1 antitrypsin (A1AT) which, after carbonylation, undergoes a conformational change leading to protein dysfunction. Its involvement in the progression of CCA has been suggested [13]. A1AT, present in human serum, is a secretory glycoprotein and a typical serine proteinase inhibitor. Additionally, A1AT can have broader functions such as anti-oxidant activity by oxidation with oxidizing agents and anti-inflammatory properties to the regulation of neutrophil-mediated lung inflammation. A1AT can also be oxidized by free radicals released from inflammatory cells, resulting in protein dysfunction. The major cause for the loss of activity is the oxidation of methionine 351 and 358 residues, a reaction incriminated in many diseases [14]. In addition, the oxidized A1AT (ox-A1AT) leads to the imbalance between A1AT and proteases, which can cause tissue damage and could play a role in the pathogenesis of inflammatory chronic degenerative diseases [15].

Since CCA development is associated with chronic inflammation caused by liver fluke infection, consequently free radicals are released resulting in oxidative/nitrative stress and oxidation of biomolecules, including proteins. The amino acid residues at an active site of A1AT are easily damaged and ox-A1AT can be secreted into blood circulation. To further support this hypothesis; in this study we determined the expression of A1AT and ox-A1AT in human CCA tissue specimens. We also measured ox-A1AT levels in serum of CCA patients, and in high risk groups for CCA development that included patients with *O. viverrini* infection and patients with advanced periductal fibrosis (APF). The use of serum ox-A1AT as a potential risk marker to predict *O. viverrini*-associated hepatobiliary diseases as well as CCA was evaluated.

Materials and methods

Human CCA tissue and serum specimens

The paraffin-embedded CCA tissues and sera of patients (n=42) were obtained from the biospecimen bank of the Liver Fluke and Cholangiocarcinoma Research Center, Faculty of Medicine at Khon Kaen University. Samples with other disease conditions related to inflammation, including hepatoma (n=8), acute cholangiohepatitis (n=1), cystadenocarcinoma (n=1), chronic bile duct dilation (n=1), chronic inflammation (n=12), ascending cholangitis (n=1), acute pancreatitis (n=1), focal and diffused inflammatory reaction of the gall bladder (n=3), granulomatous inflammation (n=2) and chronic hepatitis (n=2) were also recruited for this study. All surgical tissue samples were histopathogically ascertained.

Sera were obtained from subjects living in the Phu Wiang district, nearby Khon Kaen, Thailand. They were collected from the following groups: (1) healthy controls (n=20), with no history of *O. viverrini* infection as proven by negative test results for *O. viverrini* antibody and the absence of parasite eggs in feces; (2) group of *O. viverrini*-infected patients without periductal fibrosis (n=38) who were positive for *O. viverrini*-egg count (<1,000 epg) and its antibody; (3) heavily *O. viverrini* infected patients (egg count >1,000 epg, n=5); and (4) patients with APF (n=27). Subjects with or without periductal fibrosis were examined by abdominal ultrasonography. Grading of the fibrosis was defined as follows: grade 0 when no echoes were observed in any segment of the liver; 1+ when echoes were observed in one segment; 2+ when echoes were observed in two or three segments and 3+ when echoes were observed in more than three segments. APF patients were defined when the ultrasound grading was grade 2+ and 3+ [16]. Obese, diabetic and patients with chronic viral hepatitis infection and tuberculosis were excluded from the study. In addition, to exclude urinary tract infection and/or related inflammatory diseases, we tested the morning urine of all subjects for the presence nitrate/nitrite by using urinary test kits. Positive results were also part of the exclusion criteria.

The protocol of collection and study design were approved by Ethic Committee for Human Research, Khon Kaen University (HE551303). Informed consent was obtained from each subject. Biological samples were kept frozen at −20 °C until use. The characteristics of study participants are listed in Table 1.

Immunohistochemical detection of A1AT and ox-A1AT in CCA tissue samples

The paraffin embedded CCA tissues were deparaffinized and rehydrated with stepwise decreasing concentration of ethanol. The sections were then submerged into 10 mM citrate buffer pH 6.0 under high power (800 W) for 10 min, then sections were immersed for 30 min in 3 % (v/v) hydrogen peroxide for endogenous hydrogen peroxide activity blocking and non-specific binding was blocked by 5 % bovine serum albumin (BSA) for 30 min. Sections were then incubated with the primary antibody specific to A1AT (Abcam Plc, Cambridge, UK) or ox-A1AT (Ikagaku Co. Ltd, Kyoto, Japan) followed by peroxidase conjugated secondary antibody. After that, the color was developed with 3,3′-diaminobenzidine tetrahydrochloride (DAB) as substrate and then counterstained with Mayer's hematoxylin. The staining frequency of A1AT and ox-A1AT was semiquantitatively scored based on the percentage of positive cells as: 0 %=negative; 1–25 %=+1; 26–50 %=+2; and >50 %=+3. The staining intensity in tumor cells was scored as weak=1, moderate=2 and strong=3. Low and high expression scores were calculated by multiplying the frequency score with intensity score, and was classified into three categories: 0, negative; 1–3, low expression; 4–9, high expression.

Double-immunofluorescence assay for A1AT and ox-A1AT

The co-localization of A1AT and ox-A1AT in CCA tissues was investigated by double-immunofluorescence technique. In brief, sections were incubated with mouse anti-ox-A1AT and rabbit anti-A1AT antibody, followed by incubation with Alexa 488 donkey anti-rabbit IgG and Alexa 555 donkey anti-mouse IgG (Invitrogen, California, USA) using a fluorescence microscope for analysis (Carl Zeiss, Germany).

ELISA methods for ox-A1AT detection

For the sandwich ELISA procedure, 96-well microtiter plates were coated with anti-A1AT antibody at a dilution of 1:8,000 in coating buffer (0.05 M carbonate buffer, pH 9.6) and kept overnight at 4 °C. The plates were then washed with washing buffer and uncoated sites were blocked with a solution of 5 % BSA in PBS. After incubation for 1 h at 37 °C, wells were emptied, washed and loaded with serum samples at a dilution of 1:100 and incubated at 37 °C for 1 h. After washing, wells were loaded with ox-A1AT antibody at a dilution of 1:500 and incubated at 37 °C for 2 h. Then, peroxidase-conjugated goat anti-mouse IgG (dilution 1:2,500; Bio-Rad, USA) was added and incubated for 45 min at 37 °C. The plates were washed and incubated with a substrate *o*-phenylenediamine dihydrochloride (OPD) (Zymed, California, USA) for 30 min at room temperature, and the optical density (OD) was measured at 492 nm with an ELISA reader (Tecan Sunrise Absorbance Reader, Austria).

The concentration of serum ox-A1AT was analyzed by indirect ELISA. The plates were coated with 100 μl serum samples at a dilution of 1:100 and incubated overnight at 4 °C. Then, wells were blocked by 5 % BSA for 1 h at 37 °C. After washing, 100 μl of diluted primary antibody were added and incubated for 2 h at 37 °C. After washing, 100 μl of goat anti mouse IgG-HRP (Bio-Rad, USA) were added and incubated for 45 min at 37 °C. Then, wells were washed and incubated with 100 μl of OPD substrate for 30 min at room temperature. The reaction was stopped with 100 μl of 4 N H_2SO_4 and measured on an ELISA reader at the absorbance of 490 nm.

Additionally, the concentration of serum A1AT was determined by sandwich ELISA using commercial sandwich ELISA kit (GenWay Biotech, Inc., USA) according to the manufacturer's instructions.

Table 1 Characteristics of study subjects

Characteristics	Healthy (%)	*O. viverrini* infection without fibrosis <1,000 epg (%)	*O. viverrini* infection without fibrosis >1,000 epg (%)	APF (%)	Other diseases (%)	CCA (%)
Total (*n*)	20	33	5	27	32	42
Sex						
Male	6 (30.0 %)	19 (57.6 %)	2 (40.0 %)	18 (66.7 %)	23 (71.9 %)	26 (61.9 %)
Female	14 (70.0 %)	14 (42.4 %)	3 (60.0 %)	9 (33.3 %)	9 (28.1 %)	16 (38.1 %)
Age (years)						
20–29	0 (0.0 %)	0 (0.0 %)	0 (0.0 %)	1 (3.7 %)	0 (0.0 %)	0 (0.0 %)
30–39	0 (0.0 %)	4 (12.1 %)	1 (20.0 %)	4 (14.8 %)	0 (0.0 %)	2 (4.8 %)
40–49	6 (30.0 %)	15 (45.5 %)	1 (20.0 %)	3 (11.1 %)	7 (21.9 %)	4 (9.5 %)
≥50	14 (70 %)	14 (42.4 %)	3 (60 %)	19 (70.4 %)	25 (78.1 %)	36 (85.7 %)

Statistical analysis

Statistical analyses were performed using SPSS software V.15. Data are represented as mean±SD. The association of A1AT and ox-A1AT expression in tissues and clinical–pathological data of patients were analyzed by Fisher's exact test. Survival curves were calculated according to the Kaplan and Meier method. The diagnostic performance of ox-A1AT was evaluated using a receiver operating characteristic (ROC) curve analysis, and area under the ROC curve (AUC) with 95 % (CI) was calculated and then the optimal cut-off OD value for ox-A1AT levels were selected to balance sensitivity and specificity. Odds ratios (OR) were calculated to determine the association between cross-sectional data to predict the possible risk factors and disease outcome. Correlations between serum A1AT and ox-A1AT level in all groups were determined by calculating Pearson's correlation coefficients. A P value <0.05 was considered statistically significant.

Results

Immunohistochemical analysis of A1AT and ox-A1AT in human CCA tissues

The mean age of the 42 CCA patients under study (27 males and 15 females) was 57.2±9.5 years (range, 37–82 years). Immunoreactivity of both A1AT and ox-A1AT was restricted to the cytoplasm in all positive cases. The expression of both proteins was higher in tumor cells and was only weakly expressed in normal bile duct epithelia (Fig. 1a). Immunohistochemical staining for A1AT showed high expression in 24 cases (57.1 %) and high expression of ox-A1AT in 20 cases (47.6 %) of CCA patients. Table 2 shows that 18 cases (42.9 %) showed high expression of both forms and 16 cases (38.1 %) low expression being statistically significant ($P<0.001$). Neither an increased level of A1AT nor ox-A1AT was associated with age, gender or histological grading. No difference was found between the level of A1AT and survival time. However, high expression of ox-A1AT levels in tumor tissues significantly correlated with poor prognosis ($P=0.031$) (Fig. 1b).

Co-localization of ox-A1AT and A1AT in CCA tissues

The localization of A1AT and ox-A1AT in CCA tissue was compared as shown in Fig. 1c. The cellular compartments containing A1AT (green) and ox-A1AT (red) were similar. Our results demonstrated that these proteins co-localized (yellow) in the cytoplasm. Interestingly, some A1AT was oxidized and appeared as ox-A1AT form.

Detection of ox-A1AT by sandwich ELISA in serum

Serum ox-A1AT levels in the groups investigated are presented in Fig. 2a as box and whisker plots. CCA patients had significantly higher serum ox-A1AT level than other groups with inflammation-related diseases ($P<0.001$). CCA patients showed no differences as compared to healthy controls. However, the increase vs. controls of ox-A1AT levels in APF patients ($P<0.001$), in subjects with *O. viverrini* infection >1,000 epg ($P<0.001$) and in patients with other diseases ($P<0.001$) was significant in all three groups. Area under the ROC curve (AUC) between APF patients and healthy subjects was 0.716 (95 % CI, 0.565–0.838; $P=0.003$) which was significantly higher than cut-off value (0.5) (Fig. 2b). For CCA vs. controls the AUC value was 0.581 (95 % CI, 0.449–0.705 $P>0.05$) (Fig. 2c). The sensitivity and specificity of the serum ox-A1AT level for identifying APF were 85.1 % and 55 % and those for detecting CCA were 35.7 % and 90 %, respectively (Table 3).

Detection of serum ox-A1AT by indirect ELISA

Indirect ELISA was used to compare ox-A1AT detection with sandwich ELISA in serum. Ox-A1AT level in CCA was significantly different from *O. viverrini* infected subjects without fibrosis and from healthy controls (all $P<0.001$) (Fig. 2d). Moreover, ox-A1AT levels in sera of CCA cases, of patients with APF or other diseases, and in the group of *O. viverrini* infection >1,000 epg were much higher than in healthy controls (all $P<0.001$). To evaluate the diagnostic OD value of serum ox-A1AT level, the ROC curve was constructed based on the sensitivity and specificity of the biomarker at different cut-off points, so to differentiate APF and CCA patients from healthy subjects. The AUC value for identifying APF was 0.983 (95 % CI, 0.894–0.996; $P<0.001$) (Fig. 2e). The best cut-off OD value of serum ox-A1AT level for identifying APF was 0.209 ($P<0.001$). The sensitivity and specificity at this cut-off value were 96.3 % and 90 %, respectively. AUC between CCA and healthy controls was 0.818 (95 % CI, 0.699–0.904; $P<0.001$) (Fig. 2f), and the cut-off OD value was 0.12 ($P<0.001$), yielding a high sensitivity and specificity of 81 % and 80 %, respectively (Table 4). Additionally, we measured serum A1AT levels using commercial sandwich ELISA kits, no difference was found between the groups studied (data not shown).

Predictive values of serum ox-A1AT level measured by indirect ELISA for diagnosis of CCA

The efficacy of serum ox-A1AT level measured by indirect ELISA for screening of CCA based on the optimal cut-off

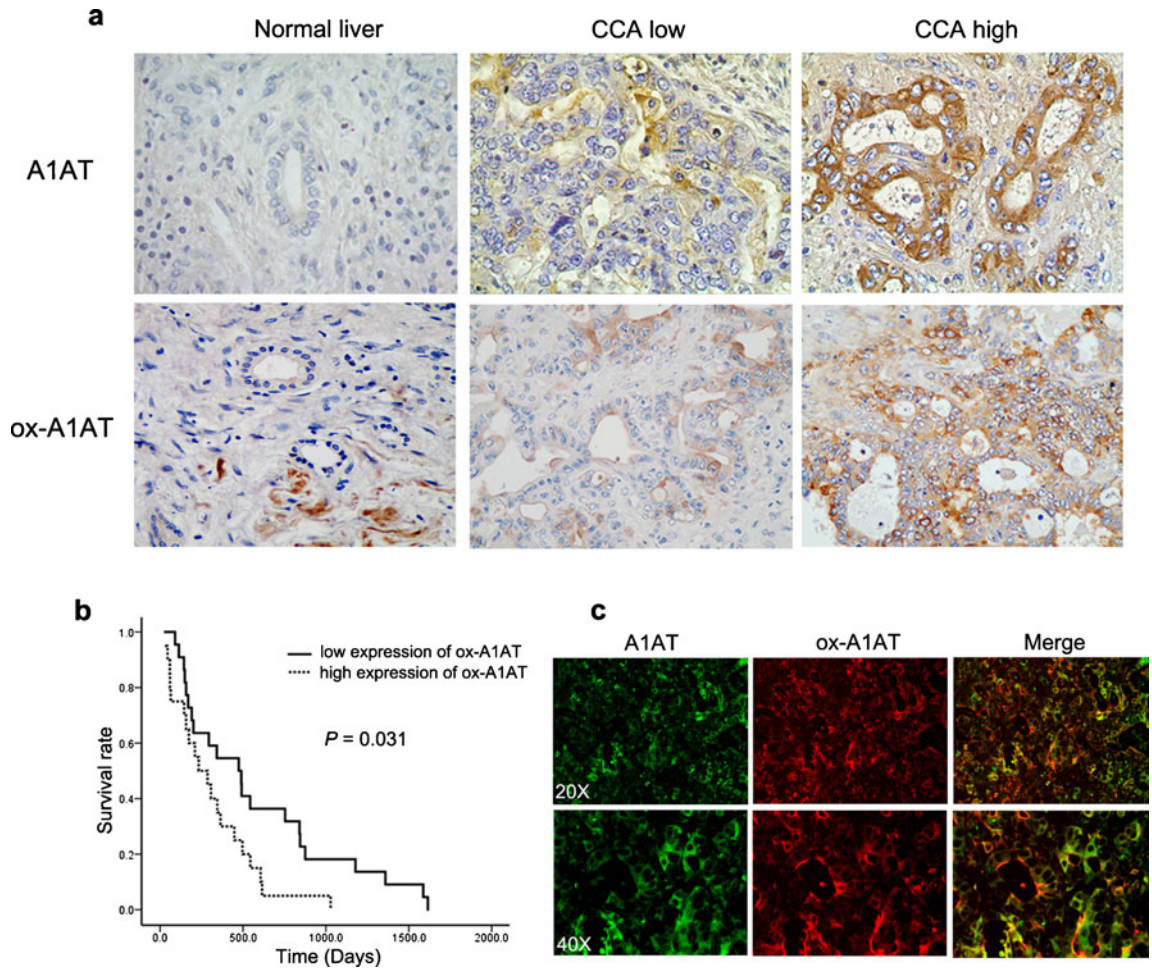

Fig. 1 Immunohistochemistry of A1AT (*upper panels*) and ox-A1AT (*lower panels*) in CCA tissues. The expressions of both proteins were higher in tumor cells whereas it was weakly expressed in normal bile duct epithelia from cadaveric donors. **a** The expression level of A1AT and oxidized A1AT in CCA cases were classified as low and high levels according to the staining intensity and frequency score. Original magnification is ×40. **b** The survival curves calculated for ox-A1AT according to Kaplan–Meier, with a log-rank test (P=0.031). **c** Co-localization of A1AT and ox-A1AT by double-immunofluorescence. Original magnification: ×20 and ×40. (*CCA low* low expression of A1AT and ox-A1AT in CCA tissue; *CCA high* high expression of A1AT and ox-A1AT in CCA tissue)

obtained from ROC analysis is presented in Table 4. ROC curve analysis revealed that the ox-A1AT level could be used to distinguish between the following groups: healthy subjects and heavy *O. viverrini* infection (P<0.001, AUC=0.950), healthy and APF (P<0.001, AUC=0.983), healthy and other diseases (P<0.001, AUC=0.913) and healthy and CCA (P<0.001, AUC=0.818). The ox-A1AT levels between paired subjects of other disease groups were also analyzed but revealed no statistical significance.

Table 2 Grading of A1AT and ox-A1AT expression in high and low in the same CCA sample

ox-A1AT expression	A1AT expression	
	Low	High
Low	16 cases (38.1 %)*	6 cases (14.3 %)
High	2 cases (4.8 %)	18 cases (42.9 %)*

*P<0.001 (Fisher's exact test)

Predictive risk values (OR) of ox-A1AT levels for APF and CCA

In order to determine whether high levels of ox-A1AT could be used to predict the risk for CCA, we calculated crude and adjusted odds ratios (Table 5). A high ox-A1AT level was a significant predictor to distinguish healthy subjects from APF group (OR crude=104, OR adjusted=140.5; P<0.001), healthy from CCA group (OR crude=17, OR adjusted=22, P<0.001). Importantly, high ox-A1AT could discriminate healthy from APF and CCA (OR crude=15.71; P<0.001, OR adjusted=22.38; P<0.001).

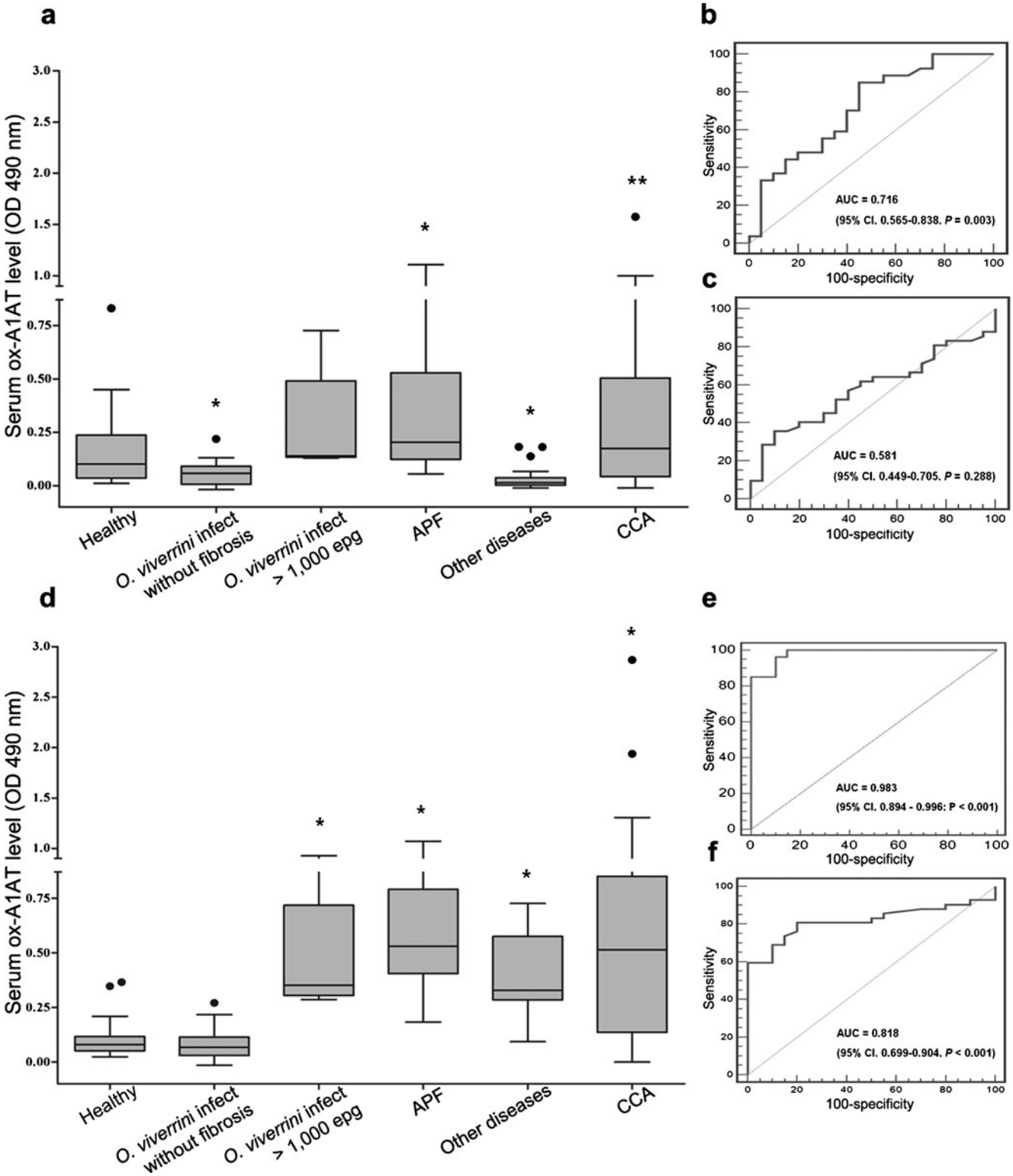

Fig. 2 The distribution of serum ox-A1AT level each group is shown in box and whisker plots. Data are representative as mean ± SD. *Significantly higher than the healthy group ($P<0.001$), **significantly higher than other diseases ($P<0.001$), but not different between themselves (Student's *t*-test). **a** Ox-A1AT level was determined by sandwich ELISA. ROC curves in patients with APF to healthy subjects (**b**) and CCA to healthy (**c**) were constructed. Serum ox-A1AT was also analyzed by using indirect ELISA (**d**) and ROC curves in patients with APF and CCA to compare with healthy group were represented in **e** and **f**, respectively. Area under ROC curve (*AUC*) and statistic comparison are indicated

Table 3 Performances of serum ox-A1AT detection by ELISA for diagnosis of APF and CCA

Comparative diagnosis	Method	Cut-off OD	Sensitivity (95 % CI)	Specificity (95 % CI)	PLR (95 % CI)	NLR (95 % CI)	*P* value
Healthy vs. APF	sELISA	>0.105	85.1 (66.3–93.7)	55 (31.6–76.9)	1.89 (1.1–3.2)	0.27 (0.1–0.7)	0.004
	iELISA	>0.209	96.3 (81.0–99.4)	90 (68.3–98.5)	9.63 (2.6–35.9)	0.04 (0.0–0.3)	<0.001
Healthy vs. CCA	sELISA	>0.327	35.7 (21.6–52.0)	90 (68.3–98.8)	3.57 (2.3–5.5)	0.71 (0.2–2.7)	0.289
	iELISA	>0.120	81 (65.9–91.4)	80 (56.3–94.3)	4.05 (3.1–5.3)	0.24 (0.1–0.7)	<0.001

sELISA sandwich ELISA, *iELISA* indirect ELISA, *95 % CI* confidence interval, *PLR* likelihood ratio for a positive result, *NLR* likelihood ratio for a negative result

Correlation between A1AT and ox-A1AT in serum of CCA patients

Analysis of A1AT and ox-A1AT levels in serum by linear regression (Fig. 3) revealed that ox-A1AT was negatively correlated with A1AT ($r=-0.586$, $P<0.001$). The decrease in serum A1AT reflects its progressive oxidation to ox-A1AT which we have detected in serum of CCA patients.

Discussion

This is the first study to demonstrate an A1AT and ox-A1AT overexpression in surgical CCA tissue sample. Immunohistochemical analysis revealed that A1AT and ox-A1AT was weakly present in normal bile duct epithelial whereas their expression was significantly increased in tumor cells. No correlations were found with age, gender, histological type and metastasis stage in the CCA patients. Cumulative survival analysis demonstrated that CCA patients with high expression of ox-A1AT had a significantly poorer prognosis ($P=0.03$). These data further support that high ox-A1AT is associated with CCA progression, leading to an accumulation of oxidized proteins as a consequence of excess of oxidative stress during *O. viverrini*-related cholangiocarcinogenesis. We also observed a co-localization of A1AT and ox-A1AT in human CCA tissues by double-immunofluorescence. Figure 1c demonstrates that some A1AT was oxidized and appeared as ox-A1AT.

One of the most difficult tasks in treating CCA is a lack of effective tests to diagnose and screen for patients with CCA. The current early detection of CCA is an important way to decrease mortality rate. Recently, there are reports demonstrated that platelet-derived growth factor alpha (PDGFA) [17] and extracellular protein kinase A (ECPKA) autoantibody [18] are involved in the tumorigenesis of CCA and possibly be a biomarker for diagnosis and predicting the risk of CCA, respectively. Various markers such as CEA and CA 19-9 are common tumor markers used for detecting CCA. Their sensitivity is low because they can be elevated in the setting of other gastrointestinal or other bile duct pathologies [19]. In our series, we found that the sensitivity was 81 % and the specificity was 80 % for serum ox-A1AT level. Moreover, we have evaluated and compared sandwich and indirect ELISA for the detection of ox-A1AT in serum. The indirect test had a greater sensitivity than sandwich test (81 % and 35.7 %, respectively) to distinguish CCA from healthy and specificity of them were 80 % and 90 %, respectively. In addition, indirect ELISA was higher both of sensitivity and specificity when compared with sandwich ELISA to differentiate APF from healthy (Table 2). The level of ox-A1AT in healthy control was higher than *O. viverrini* infected group, one

Table 4 Predictive values of serum ox-A1AT levels measured by indirect ELISA for diagnosis of APF and CCA, based on the cut-off points obtained from ROC analysis

Group comparisons	AUC (95 % CI)	Cut-off OD	Sensitivity	Specificity	*P* value
Healthy vs. APF	0.983 (0.894–0.996)	0.209	96.3	90.0	<0.001
Healthy vs. CCA	0.818 (0.699–0.904)	0.120	81.0	80.0	<0.001
Healthy vs. *O. viverrini*-infection (>1,000 epg)	0.950 (0.782–0.998)	0.209	100.0	90.0	<0.001
Healthy vs. other diseases	0.913 (0.825–0.982)	0.140	96.9	85.0	<0.001
Healthy vs. *O. viverrini* infection without fibrosis	0.586 (0.449–0.713)	0.065	50.0	70.0	0.267
O. viverrini infection (>1,000 epg) vs. CCA	0.500 (0.351–0.649)	0.286	61.9	20.0	1.000
APF vs. CCA	0.554 (0.429–0.674)	0.236	35.7	96.3	0.440
Other diseases vs. CCA	0.568 (0.448–0.683)	0.609	47.6	87.5	0.307

AUC area under the ROC curve

Table 5 Predictive risk values (ORs) of advanced periductal fibrosis (APF) and CCA relative to healthy subjects based on serum ox-A1AT levels

Group comparisons	Crude OR	95 % CI (*P* value)	OR[a] adjusted	95 % CI (*P* value)
Healthy vs. APF				
ox-A1AT OD >0.209 vs. ≤0.209	104.00	10.65–1014.82 (<0.001)	140.52	9.93–1987.76 (<0.001)
Healthy vs. CCA				
ox-A1AT OD >0.120 vs. ≤0.120	17.00	4.45–64.87 (<0.001)	22.03	4.79–101.31 (<0.001)
Healthy vs. APF and CCA				
ox-A1AT OD >0.221 vs. ≤0.221	15.71	4.53–54.45 (0.017)	22.38	5.36–93.46 (<0.001)

OR odds ratio, *CI* confidence interval, *APF* advanced periductal fibrosis, *CCA* cholangiocarcinoma

[a] Odds ratio adjusted for age and sex statistical analysis

possible explanation is that normal controls were also living in the endemic area of liver fluke infection and some may have inflammatory condition which could not be detected in this study. Indirect ELISA differs from sandwich ELISA in that antigen is bound directly to the polystyrene surface, thus it is directly affected by the binding event. Consequently, we suggested that indirect ELISA could be as a screening method and useful as routine serum ox-A1AT detection because time and cost of analysis are considerably reduced.

Our study shows that the levels of ox-A1AT were higher in group of heavy *O. viverrini* infection, APF and CCA patients than those in *O. viverrini* infection without fibrosis and healthy subjects. This is also evidenced by the high expression of A1AT and ox-A1AT in CCA tissues. The present results indicated that ox-A1AT may lead to a conformational change and protein dysfunction. Notably, serum ox-A1AT level was increased in opisthorchiasis and correlated with fibrosis. We have also calculated the cut-off OD value of serum ox-A1AT level to distinguish and predict the risk of APF and CCA from healthy controls (Table 3). The high ox-A1AT level in healthy is predictable for APF and CCA risks ($P<0.001$; OR=140.52 and 22.03, respectively). The higher OR in APF group when compared with CCA group may be explained that ox-A1AT plays an active role during tissue remodeling and fibrosis as depicted in Fig. 4. In humans, APF may lead to hepatobiliary diseases and an increased risk of CCA development. Therefore, ox-A1AT is a potential biomarker to predict the risk of opisthorchiasis-associated CCA. The level of ox-A1AT is also detected in patients with rheumatic diseases and bronchiectasis, indicating the involvement of free radicals [20, 21]. Inactivation of A1AT with subsequently enhanced proteolysis, has been involved in the probably promotes local inflammatory processes, including uncontrolled degradation of connective tissues. Ueda and coworkers reported that the ox-A1AT was also detected in the serum of patients with inflammatory diseases, indicating the involvement of oxidative stress [22]. Previously, ox-A1AT was reported in plasma of patients with heart failure, which biological function is altered due

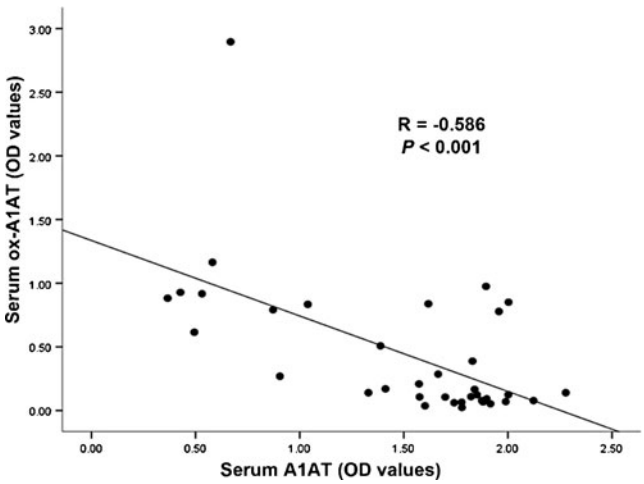

Fig. 3 Inverse correlations between A1AT and ox-A1AT levels in sera from CCA patients ($P<0.001$). The levels of serum A1AT and ox-A1AT were analyzed by sandwich ELISA and indirect ELISA, respectively

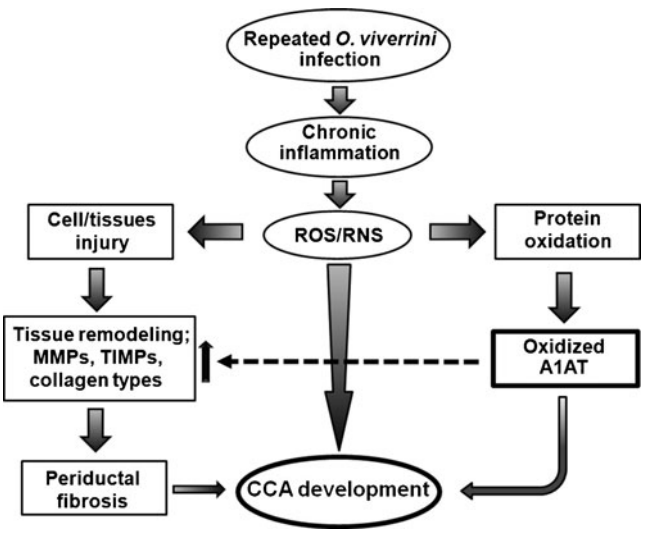

Fig. 4 A possible link of ox-A1AT in relation to *O. viverrini*-associated cholangiocarcinoma development. (*ROS* reactive oxygen species, *RNS* reactive nitrogen species, *A1AT* alpha-1 antitrypsin, *MMPs* matrix metalloproteinases, *TIMPs* tissue inhibitor of MMPs, *CCA* cholangiocarcinoma)

to endothelial damage [15]. Additionally, we examined the correlation between A1AT and ox-A1AT in serum, we found that the level of ox-A1AT was negatively correlated with A1AT level ($r=-0.586$, $P<0.001$). The evidence is supported by the report of Izumi-Yoneda et al. [23], who showed that the concentration of A1AT was decreased in the amniotic fluid, which is related to an inflammatory reaction in those cases. This may be explained by the increased level of ox-A1AT [23].

A1AT has some sulfur-containing amino acid (Met 351 and 358) residues at the active site that are most susceptible to oxidation, and also resulting in loss of serine protease inhibitory capacity [14]. Serine protease inhibitors play an important role in modulation of the inflammatory response and are involved in tumor growth and invasiveness [24, 25]. Serine proteases released by neutrophil trigger a protease cascade that entails activation of proMMP-2, an enzyme involved in tumor invasion and angiogenesis [26]. Active forms of MMP-2 and MMP-9 were high in both sera and liver tissue not only in *O. viverrini*-infected hamsters [10] but also in sera of CCA patients [27]. Taken together, our model implies that chronic inflammation induced by *O. viverrini* infection leads to protein damage, including ox-A1AT which cannot inactivate proteases activity, resulting in pro-MMPs activation. Finally, tissue remodeling and severe fibrosis occurs during opisthorchiasis-driven cholangiocarcinogenesis, thus ox-A1AT might play role in CCA development as shown in Fig. 4.

In conclusion, although further studies are required to elucidate the mechanism and role of ox-A1AT expression in CCA, we confirmed that high expression of oxidized A1AT is significantly correlated with a poorer prognosis of CCA patients. Our results indicate that serum ox-A1AT level using indirect ELISA is a potential biomarker to screen and predict the risk of opisthorchiasis-related CCA development.

Acknowledgements This study was supported by a NRU-Khon Kaen University Scholarship (to WJ and PY), Khon Kaen University Research Grant (Grant No. 550404) and the Higher Education Research Promotion and National Research University Project of Thailand, Office of the Higher Education Commission, through the Health Cluster (SHeP-GMS) Khon Kaen University. We thank Helmut Bartsch (PhD), Heidelberg, Germany, for his comments and editorial assistance.

References

1. Sriplung H, Wiangnon S, Sontipong S, Sumitsawan Y, Martin N. Cancer incidence trends in Thailand, 1989–2000. Asian Pac J Cancer Prev. 2006;7(2):239–44.
2. Parkin DM. The global health burden of infection-associated cancers in the year 2002. Int J Cancer. 2006;118(12):3030–44.
3. Sithithaworn P, Andrews RH, Nguyen VD, Wongsaroj T, Sinuon M, Odermatt P, et al. The current status of opisthorchiasis and clonorchiasis in the Mekong Basin. Parasitol Int. 2012;61(1):10–6.
4. Yongvanit P, Pinlaor S, Bartsch H. Oxidative and nitrative DNA damage: key events in opisthorchiasis-induced carcinogenesis. Parasitol Int. 2012;61(1):130–5.
5. Yongvanit P, Thanan R, Pinlaor S, Sithithaworn P, Loilome W, Namwat N, et al. Increased expression of TLR-2, COX-2, and SOD-2 genes in the peripheral blood leukocytes of opisthorchiasis patients induced by *Opisthorchis viverrini* antigen. Parasitol Res. 2012;110(5):1969–77.
6. Pinlaor S, Ma N, Hiraku Y, Yongvanit P, Semba R, Oikawa S, et al. Repeated infection with *Opisthorchis viverrini* induces accumulation of 8-nitroguanine and 8-oxo-7,8-dihydro-2′-deoxyguanine in the bile duct of hamsters via inducible nitric oxide synthase. Carcinogenesis. 2004;25(8):1535–42.
7. Pinlaor S, Sripa B, Sithithaworn P, Yongvanit P. Hepatobiliary changes, antibody response, and alteration of liver enzymes in hamsters re-infected with *Opisthorchis viverrini*. Exp Parasitol. 2004;108(1–2):32–9.
8. Boonmars T, Srisawangwong T, Srirach P, Kaewsamut B, Pinlaor S, Sithithaworn P. Apoptosis-related gene expressions in hamsters re-infected with *Opisthorchis viverrini* and re-treated with praziquantel. Parasitol Res. 2007;102(1):57–62.
9. Boonmars T, Srirach P, Kaewsamut B, Srisawangwong T, Pinlaor S, Pinlaor P, et al. Apoptosis-related gene expression in hamster opisthorchiasis post praziquantel treatment. Parasitol Res. 2008;102(3):447–55.
10. Prakobwong S, Pinlaor S, Yongvanit P, Sithithaworn P, Pairojkul C, Hiraku Y. Time profiles of the expression of metalloproteinases, tissue inhibitors of metalloproteases, cytokines and collagens in hamsters infected with *Opisthorchis viverrini* with special reference to peribiliary fibrosis and liver injury. Int J Parasitol. 2009;39(7):825–35.
11. Mairiang E, Elkins DB, Mairiang P, Chaiyakum J, Chamadol N, Loapaiboon V, et al. Relationship between intensity of *Opisthorchis viverrini* infection and hepatobiliary disease detected by ultrasonography. J Gastroenterol Hepatol. 1992;7(1):17–21.
12. Mairiang E, Laha T, Bethony JM, Thinkhamrop B, Kaewkes S, Sithithaworn P, et al. Ultrasonography assessment of hepatobiliary abnormalities in 3359 subjects with *Opisthorchis viverrini* infection in endemic areas of Thailand. Parasitol Int. 2012;61(1):208–11.
13. Thanan R, Oikawa S, Yongvanit P, Hiraku Y, Ma N, Pinlaor S. Inflammation-induced protein carbonylation contributes to poor prognosis of cholangiocarcinoma. Free Rad Biol Med. 2012.
14. Taggart C, Cervantes-Laurean D, Kim G, McElvaney NG, Wehr N, Moss J, et al. Oxidation of either methionine 351 or methionine 358 in alpha 1-antitrypsin causes loss of anti-neutrophil elastase activity. J Biol Chem. 2000;275(35):27258–65.
15. Banfi C, Brioschi M, Barcella S, Veglia F, Biglioli P, Tremoli E, et al. Oxidized proteins in plasma of patients with heart failure: role in endothelial damage. Eur J Heart Fail. 2008;10(3):244–51.
16. Sripa B, Mairiang E, Thinkhamrop B, Laha T, Kaewkes S, Sithithaworn P, et al. Advanced periductal fibrosis from infection with the carcinogenic human liver fluke *Opisthorchis viverrini* correlates with elevated levels of interleukin-6. Hepatology. 2009;50(4):1273–81.
17. Boonjaraspinyo S, Boonmars T, Wu Z, Loilome W, Sithithaworn P, Nagano I, et al. Platelet-derived growth factor may be a potential diagnostic and prognostic marker for cholangiocarcinoma. Tumour Biol. 2012;33(5):1785–802.
18. Loilome W, Yooyuen S, Namwat N, Sithithaworn P, Puapairoj A, Kano J, et al. PRKAR1A overexpression is associated with increased ECPKA autoantibody in liver fluke-associated cholangiocarcinoma: application for assessment of the risk group. Tumour Biol. 2012;33(6):2289–98.

19. Van Beers BE. Diagnosis of cholangiocarcinoma. HPB (Oxford). 2008;10(2):87–93.
20. Chidwick K, Winyard PG, Zhang Z, Farrell AJ, Blake DR. Inactivation of the elastase inhibitory activity of alpha 1 antitrypsin in fresh samples of synovial fluid from patients with rheumatoid arthritis. Ann Rheum Dis. 1991;50(12):915–6.
21. Sepper R, Konttinen YT, Ingman T, Sorsa T. Presence, activities, and molecular forms of cathepsin G, elastase, alpha 1-antitrypsin, and alpha 1-antichymotrypsin in bronchiectasis. J Clin Immunol. 1995;15(1):27–34.
22. Ueda M, Mashiba S, Uchida K. Evaluation of oxidized alpha-1-antitrypsin in blood as an oxidative stress marker using anti-oxidative alpha1-AT monoclonal antibody. Clin Chim Acta. 2002;317(1–2):125–31.
23. Izumi-Yoneda N, Toda A, Okabe M, Koike C, Takashima S, Yoshida T, et al. Alpha 1 antitrypsin activity is decreased in human amnion in premature rupture of the fetal membranes. Mol Hum Reprod. 2009;15(1):49–57.
24. Mannello F, Gazzanelli G. Tissue inhibitors of metalloproteinases and programmed cell death: conundrums, controversies and potential implications. Apoptosis. 2001;6(6):479–82.
25. Remacle A, McCarthy K, Noel A, Maguire T, McDermott E, O'Higgins N, et al. High levels of TIMP-2 correlate with adverse prognosis in breast cancer. Int J Cancer. 2000;89(2):118–21.
26. Shamamian P, Schwartz JD, Pocock BJ, Monea S, Whiting D, Marcus SG, et al. Activation of progelatinase A (MMP-2) by neutrophil elastase, cathepsin G, and proteinase-3: a role for inflammatory cells in tumor invasion and angiogenesis. J Cell Physiol. 2001;189(2):197–206.
27. Leelawat K, Sakchinabut S, Narong S, Wannaprasert J. Detection of serum MMP-7 and MMP-9 in cholangiocarcinoma patients: evaluation of diagnostic accuracy. BMC Gastroenterol. 2009;9:30.